

Thermoelectric performance optimization of n-type PbTe by In and Cu₂Te co-doping and anomalous temperature-dependent transports

Feng Gao ^{a,b,1}, Jianfeng Cai ^{b,c,1}, Mancang Li ^d, Zhiyu Chen ^d, Yu Wang ^d, Zongwei Zhang ^b, Lulu Chen ^b, Ding Hu ^b, Xiaojian Tan ^{b,c}, Jiehua Wu ^b, Guoqiang Liu ^{b,c*}, Zhenhua Ge ^{a*}, Jun Jiang ^{b,c*}

a Faculty of Materials Science and Engineering, Kunming University of Science and Technology, Kunming 650093, China

b Ningbo Institute of Materials Technology and Engineering, Chinese Academy of Sciences, Ningbo 315201, China

c University of Chinese Academy of Sciences, Beijing, 100049, China

d. Science and Technology on Reactor System Design Technology Laboratory, Nuclear Power Institute of China, Chengdu 610213, China

*Corresponding authors, 1These authors contributed equally

E-mail: liugq@nimte.ac.cn, zge@kust.edu.cn, jjun@nimte.ac.cn

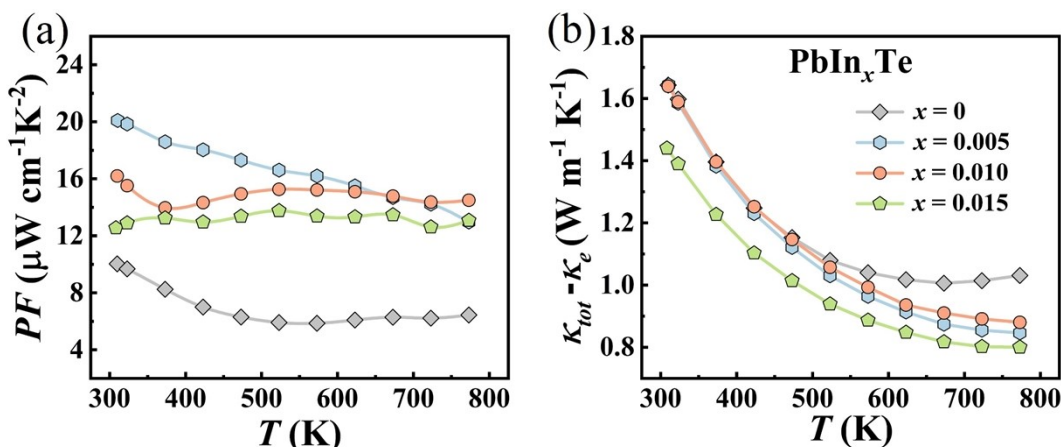


Figure S1. Temperature dependence of (a) PF , (b) lattice thermal conductivity κ_l for *n*-type PbIn_xTe ($x = 0, 0.005, 0.01, 0.015$).

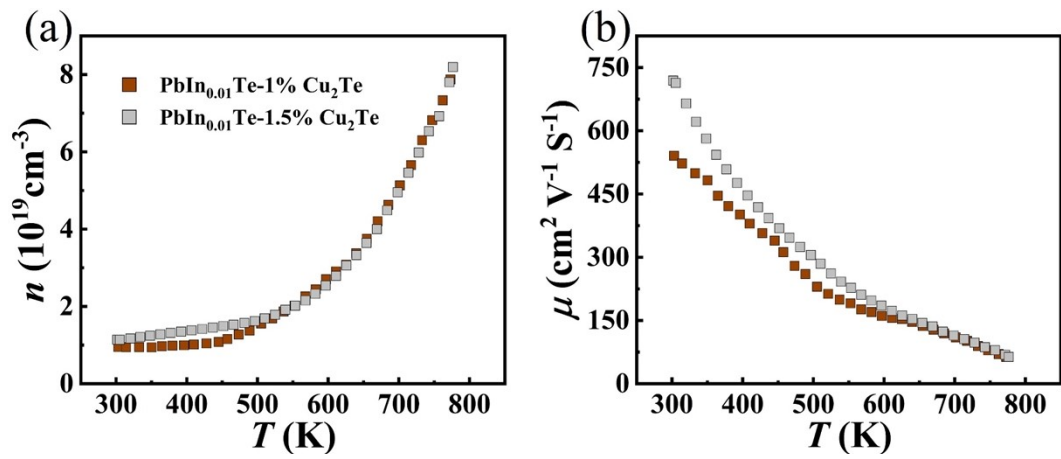


Figure S2. Temperature dependence of (a) carrier concentration, (b) carrier mobility for $\text{PbIn}_{0.01}\text{Te}-y\%\text{Cu}_2\text{Te}$ ($y = 1$, and 1.5)

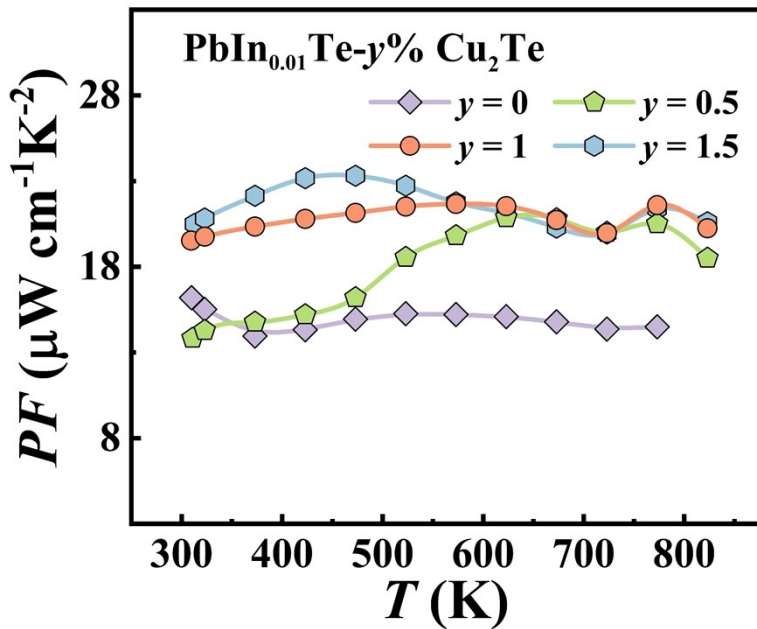


Figure S3. Temperature-dependent PF for n -type $\text{PbIn}_{0.01}\text{Te}-y\%\text{Cu}_2\text{Te}$ ($y = 0, 0.5, 1, 1.5$)

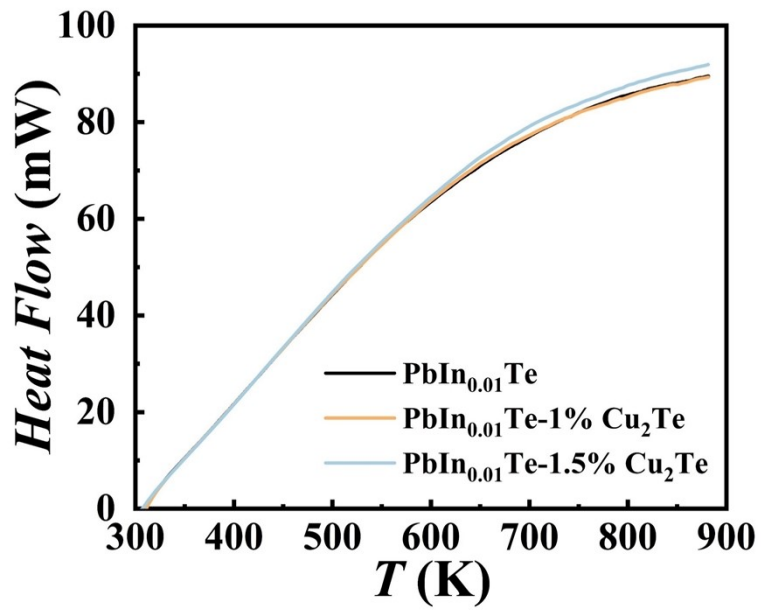


Figure S4. DSC testing of $\text{PbIn}_{0.01}\text{Te}$, $\text{PbIn}_{0.01}\text{Te}-1\% \text{Cu}_2\text{Te}$, and $\text{PbIn}_{0.01}\text{Te}-1.5\% \text{Cu}_2\text{Te}$

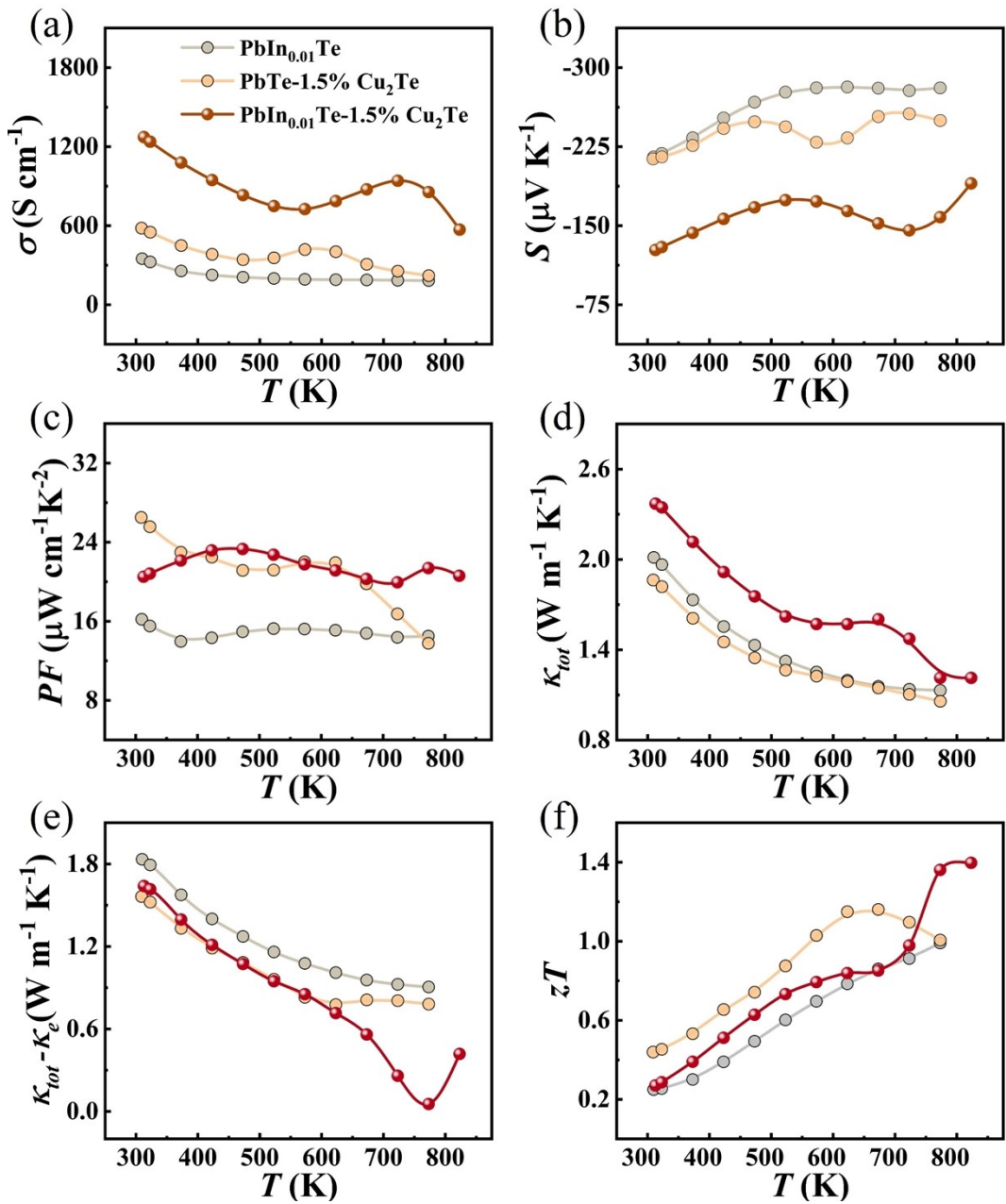


Figure S5. Temperature dependence of (a) electrical conductivity, (b) Seebeck coefficient, (c) PF , (d) total thermal conductivity κ_{tot} , (e) lattice thermal conductivity κ_l , and (f) figure of merit zT for n -type $\text{PbIn}_{0.01}\text{Te}$, $\text{PbTe-1.5\% Cu}_2\text{Te}$ and $\text{PbIn}_{0.01}\text{Te-1.5\% Cu}_2\text{Te}$.

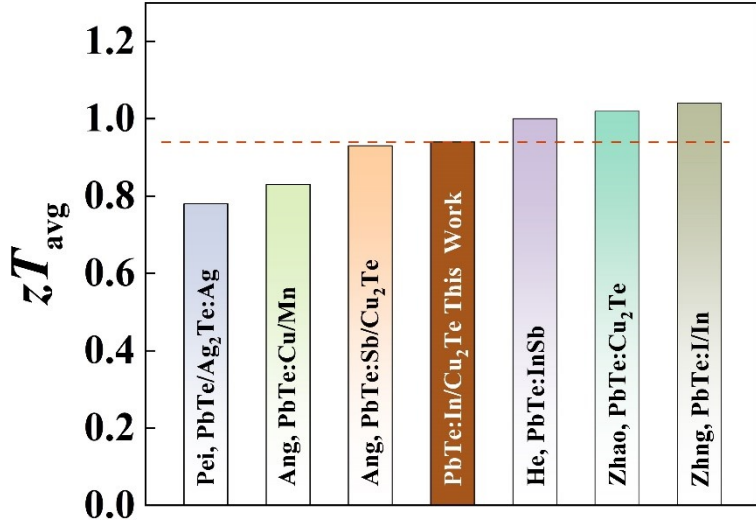


Figure S6. Compare of the corresponding zT_{avg} in this work with those of previous samples.^[1-6]

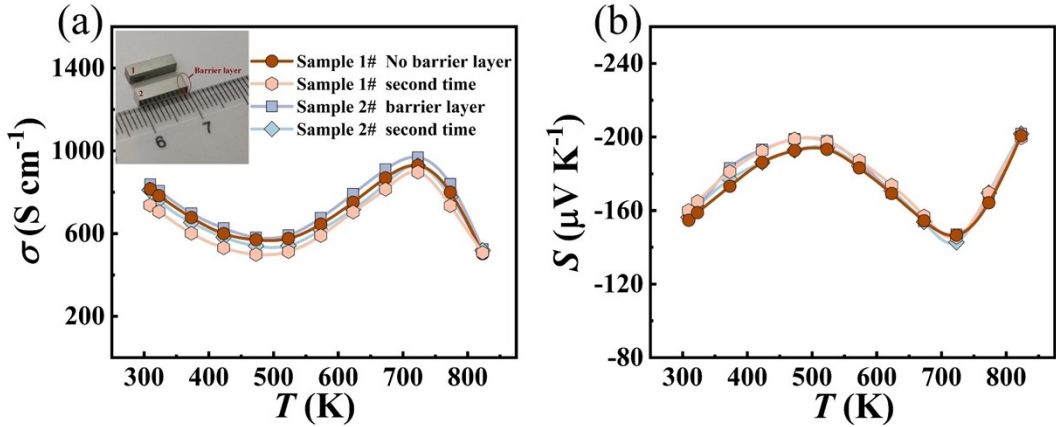


Figure S7. Temperature dependent for repeated measurements on (a) electrical conductivity, and (b) Seebeck coefficient for *n*-type $\text{PbIn}_{0.01}\text{Te}-1\%\text{Cu}_2\text{Te}$.

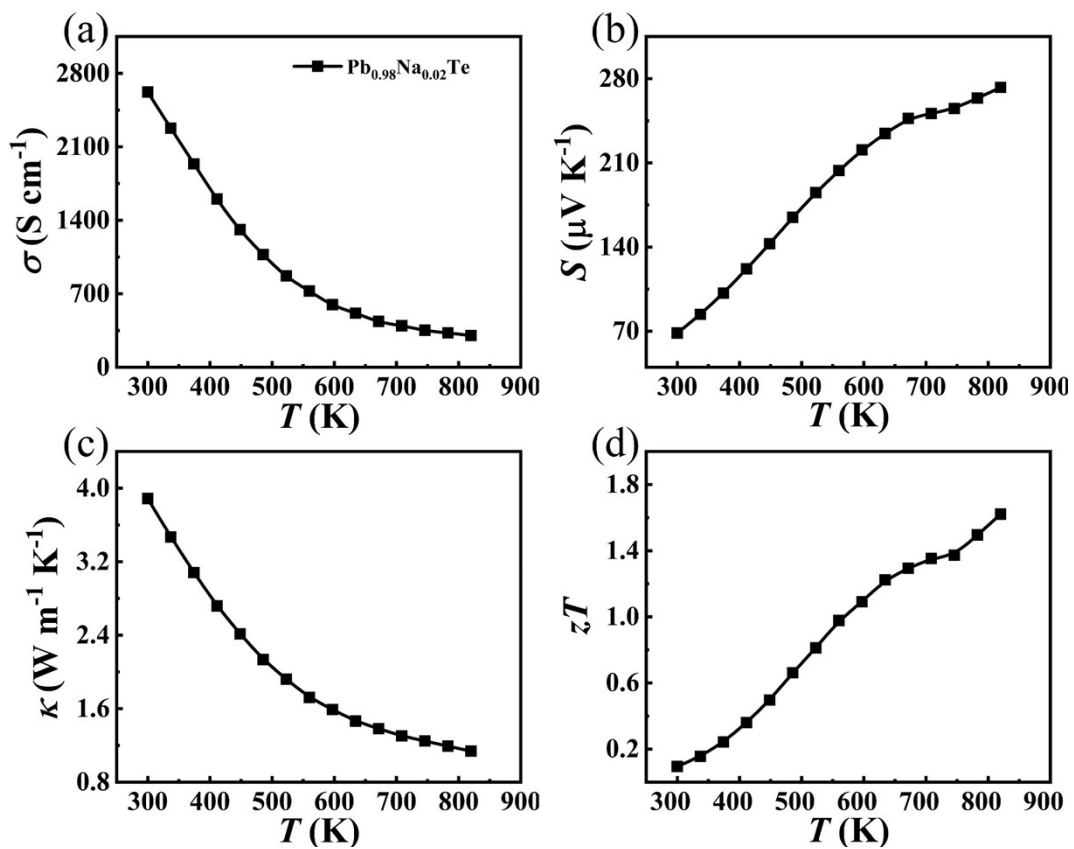


Figure S8. Temperature dependence of (a) electrical conductivity, (b) Seebeck coefficient, (c) total thermal conductivity and (d) figure of merit zT for *p*-type $\text{Pb}_{0.98}\text{Na}_{0.02}\text{Te}$.

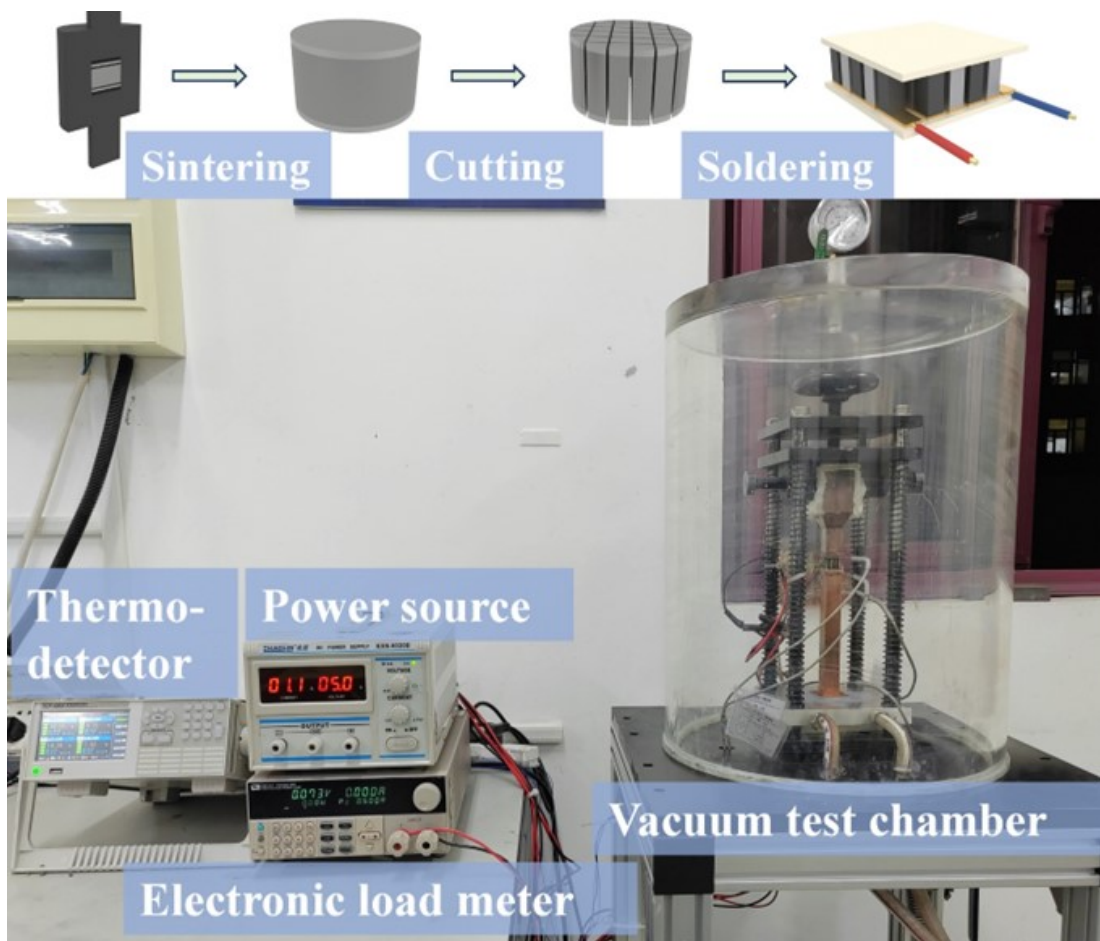


Figure S9. The flowchart of thermoelectric device preparation and home-built testing system for the thermoelectric device conversion efficiency η measurement.

Table S1 The temperature difference between the cold and hot ends of the device

T_h (K)	T_c (K)	ΔT (K)
385.6	285.26	100.34
490.34	291.09	199.25
601.18	301.55	299.63
698.56	299.5	399.06
751.94	301.64	450.30
804.15	303.55	500.60
825.81	305.78	520.03

Reference

- [1] Y. Pei, A.F. May, G.J. Snyder, Advanced Energy Materials 1 (2011) 291-296

- [2] Y. Zhong, H. Liu, Q. Deng, F. Lv, L. Gan, R. Ang, ACS Appl Mater Interfaces 13 (2021) 52802-52810
- [3] H. Liu, Z. Chen, J. Tang, Y. Zhong, X. Guo, F. Zhang, R. Ang, ACS Appl Mater Interfaces 12 (2020) 52952-52958
- [4] J. Zhang, D. Wu, D. He, D. Feng, M. Yin, X. Qin, J. He, Adv Mater 29 (2017) 1703148
- [5] Y. Xiao, H. Wu, W. Li, M. Yin, Y. Pei, Y. Zhang, L. Fu, Y. Chen, S.J. Pennycook, L. Huang, J. He, L.-D. Zhao, J Am Chem Soc 139 (2017) 18732-18738
- [6] Q. Zhang, Q. Song, X. Wang, J. Sun, Q. Zhu, K. Dahal, X. Lin, F. Cao, J. Zhou, S. Chen, G. Chen, J. Mao, Z. Ren, Energy & Environmental Science 11 (2018) 933-940